

# Temporal stability and directional change in a color cline of a marine snail from NW Spain

Juan Gefaell, Ramón Vigo , A. Honorato González-Vázquez, Juan Galindo\*\*, and Emilio Rolán-Alvarez\*\*\*

Centro de Investigación Mariña, Universidade de Vigo, Departamento de Bioquímica, Genética e Inmunología, 36310 Vigo, Spain

\*Address correspondence to Emilio Rolán-Alvarez. E-mail: [rolan@uvigo.es](mailto:rolan@uvigo.es).

\*\*These authors contributed equally to this work.

Handling editor: Zhi-Yun Jia

## Abstract

The evolution and maintenance of color clines is a classic topic of research in evolutionary ecology. However, studies analyzing the temporal dynamics of such clines are much less frequent, due to the difficulty of obtaining reliable data about past color distributions along environmental gradients. In this article, we describe a case of decades-long temporal stability and directional change in a color cline of the marine snail *Littorina saxatilis* along the coastal inlet of the Ría de Vigo (NW Spain). *L. saxatilis* from this area shows a clear color cline with 3 distinct areas from the innermost to the more wave-exposed localities of the Ría: the inner, protected localities show an abundance of fawn-like individuals; the intermediate localities show a high diversity of colors; and the outer, wave-exposed localities show populations with a high frequency of a black and lineated morph. We compare data from the 1970s and 2022 in the same localities, showing that the cline has kept relatively stable for at least over half a century, except for some directional change and local variability in the frequency of certain morphs. Multiple regression analyses and biodiversity measures are presented to provide clues into the selective pressures that might be involved in the maintenance of this color cline. Future research avenues to properly test the explanatory power of these selective agents as well as the possible origins of the cline are discussed.

**Key words:** clinal variation, color polymorphism, ecological gradient, *Littorina saxatilis*, natural selection, wave exposure.

Genetically dependent intraspecific color variation, or color polymorphism, is a common phenomenon in a wide variety of animal groups, including insects (Dearn 1990; Suárez-Tovar et al. 2022), arachnids (Oxford and Gillespie 1998), anurans (Hoffman and Blouin 2000), squamates (Abalos 2021), birds (Galeotti et al. 2003), bivalves (Cook 2017), or gastropods (Gefaell et al. 2023). A special case of color polymorphism is clines, in which there is intraspecific and geographical gradual color variation along an environmental gradient (Mayr 1963; Endler 1977; Smith and Smith 2012). Color clines can either consist of gradual changes in the intensity of a continuous color variation (e.g., going from brighter to less bright individuals), or gradual changes in the frequencies of discrete color morphs (see Davison et al. 2019 for a discussion of the continuous vs. discrete variation controversy in gastropod color polymorphism). From an evolutionary point of view, clines are normally caused by selection or neutral diffusion via interbreeding and dispersal (Sætre and Ravinet 2019), and they can be of interest to evolutionary biologists inasmuch as they can provide clues into the putative adaptive significance of color variation. Color clines have also been described in several terrestrial and marine taxa (e.g., Dearn 1981; Phifer-Rixey et al. 2008; Antoniazza et al. 2010; Cooper 2010; Takahashi et al. 2011; Köhler et al. 2017; Magnúsdóttir et al. 2018).

A particularly understudied topic in the evolutionary ecology of color clines is its temporal stability and change across prolonged periods (i.e., decades-long). So far, not many studies have systematically explored this issue, in part because it is usually hard to obtain reliable data on past dynamics of color variation (de Jong and Brakefield 1998; Cook et al. 2002; Mullen and Hoekstra 2008; Saccheri et al. 2008; Brakefield and de Jong 2011; Evans et al. 2018; Hantak et al. 2021). Particularly important in this realm are the studies conducted in the model organism *Cepaea nemoralis* (e.g., Wolda 1969; Cook and Pettitt 1998; Cook et al. 1999; Ožgo and Schlthuizen 2012; Cameron et al. 2013; Ramos-Gonzalez and Davison 2021). This kind of investigation is of uttermost importance not only because of the insights it can provide on how evolutionary forces shape biodiversity in the medium-to-long run but also because it can yield interesting information on how recent anthropogenic processes such as climate change can affect these evolutionary dynamics (e.g., de Jong and Brakefield 1998; Brakefield and de Jong 2011; Ožgo and Schlthuizen 2012; Roulin 2014; Consentino et al. 2017; Evans et al. 2018).

The rough periwinkle (*Littorina saxatilis*, Olivi 1792) is a marine gastropod species known for its high phenotypic diversity and its role as a model organism for evolutionary ecology (e.g., Johannesson 2015; Rolán-Alvarez et al.

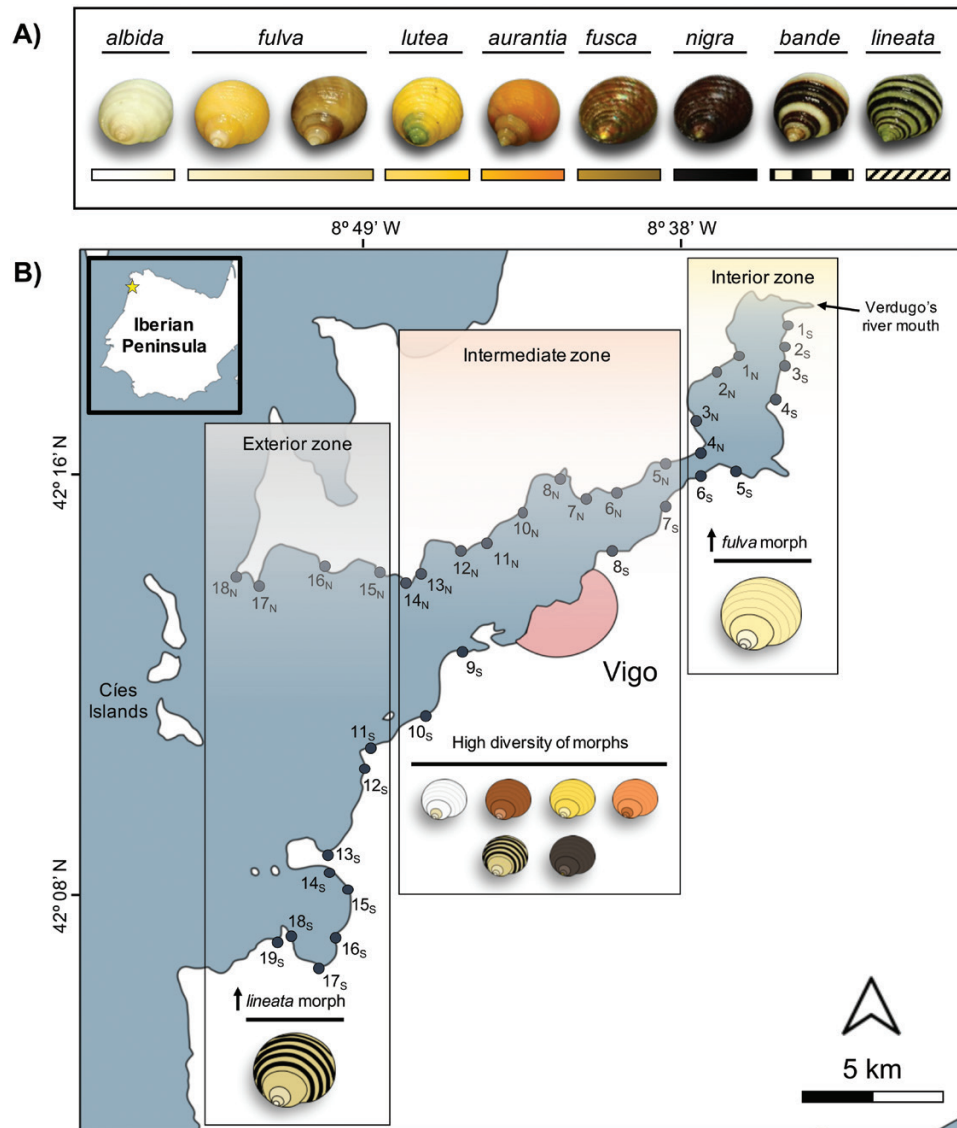


**Figure 1** (A) Color categories used by Sacchi (1979). *Tessellata* and *sanguinea* colors are not shown either because they are not representative of the composition of populations (due to low frequencies; *tessellata*) or are absent from the Ría de Vigo (*sanguinea*). (B) Color cline hypothesis for the Ría de Vigo as derived from Sacchi (1979; see also Reid 1996). According to this hypothesis, 3 different zones exist along the Ría de Vigo, each with its own color distribution: an interior zone, with high frequencies of fawn-like (“*fulva*”) individuals; an intermediate zone, with high color diversity; and an exterior zone, with high frequencies of a lineated (“*lineata*”) morph. Dots and numbers represent the different localities explored by Sacchi in 1974–1976 and re-sampled by us in 2022. Note that in the north there is a leap from 8<sub>N</sub> to 10<sub>N</sub>, as no snails were found in the 9<sub>N</sub> location (“*Moaña, entro il porto*” in Sacchi 1979; see the main text). The light pink area represents the approximate urban surface of the city of Vigo. The maps were taken and modified from d-maps (<https://www.d-maps.com>).

2015). *L. saxatilis* lives in the rocky intertidal ecosystems all over the American and European coasts of the North Atlantic Ocean, where it feeds on microalgae that grow on the surface of rocks (Reid 1996). In part due to its ovoviviparous mode of reproduction (that significantly limits its dispersal capability), as well as to the heterogeneity of the intertidal ecosystem, *L. saxatilis* shows a high tendency to evolve local adaptations and to present an enormous intraspecific phenotypic variation (reviewed in Rolán-Alvarez et al. 2015). Indeed, several different ecotypes have been described in *L. saxatilis*, among which the Crab and Wave ecotypes stand out. These ecotypes—present at least in the Swedish, British, and Spanish coasts—show specific morphological and behavioral adaptations to the different parts of the intertidal ecosystem, and molecular data show

that there exists partial reproductive isolation between them (Rolán-Alvarez 2007; Johannesson 2015; Johannesson et al. 2017).

In addition to the Crab and Wave ecotypes, of particular interest within the *L. saxatilis* system is the high diversity of color morphs that it can present (see Figure 1A). These color morphs can be found either within the same populations or between populations in geographically adjacent areas, sometimes giving rise to color clines (Reid 1996 and references therein; Gefaell et al. 2023). A region where a high diversity of color morphs of *L. saxatilis* exists is the Rías Baixas (Galicia, NW Spain). The Rías Baixas constitute a series of 4 coastal inlets that originated through the immersion of river valleys that are open to the sea (Méndez and Vilas 2005). In at least 3 out of 4 of these Rías, *L. saxatilis* presents a purported

color cline, described decades ago but not verified since then (Fischer-Piette and Gaillard 1961; Fischer-Piette et al. 1961; Sacchi 1979; Sacchi and Malcevski 1983; Reid 1996). More specifically, such a color cline would have 3 relatively well-differentiated zones: an interior zone, comprising the innermost localities closest to the mouth of the main river of each Ría, and dominated by fawn-like colors (“*fulva*”); an intermediate zone, corresponding to the midway localities of the Rías and in which high color diversity is found in terms of the number of color morphs; and an exterior zone, corresponding to the most wave exposed localities and mostly dominated by a lined (“*lineata*”) morph (see Figure 1B).

Of these 4 Rías, the Ría de Vigo (the southernmost one; with around 41 km of coast on the north and 57 km on the south) has been the most studied in the past. Sacchi (1979) analyzed the frequency of the different color morphs in several localities across this Ría, corroborating the existence of the above-mentioned color cline, previously described by Fischer-Piette and Gaillard (1961) and Fischer-Piette et al. (1961). Color-frequency data provided by Sacchi (1979), readily available within that article, constitute a unique opportunity to analyze the patterns of temporal stability and variation of a color cline in an intertidal organism. In this article, we attempt to resurvey exactly the same populations as Sacchi surveyed in the 1970s to (1) corroborate the existence of such cline; (2) determine to what extent it has changed or remained stable for the last few decades; and (3) provide a preliminary examination of the potential evolutionary mechanisms behind the medium-to-long-term dynamics of such a color cline, to come up with future ways to experimentally test their explanatory power.

## Material and Methods

### Sample collection and color assignment

In this study, 2 distinct samples were used: “1979” and “2022.” The “1979” data were taken from Sacchi’s original publication (Sacchi 1979: Tables 1–5). These localities were collectively called “1979” due to the date of Sacchi’s article, but data on such populations were collected in August–September 1974 and 1976 (Sacchi 1979). Sacchi took samples from 42 different localities across the Ría de Vigo (average  $N = 1020$ ), avoiding the urban area of the city of Vigo (see light pink area in Figure 1B). For our analyses, from these original 42 populations, 5 corresponding to Cíes Islands (an archipelago of 3 islands at the mouth of the Ría de Vigo) were excluded, as these populations do not show geographical continuity with the remaining populations. Moreover, many of these populations are associated with the Cíes Lagoon, in which a different *L. saxatilis* ecotype exists (Galindo et al. 2020), and this could confound the cline analysis. This exclusion of localities from Cíes Islands yielded a total of 37 valid localities along the Ría of Vigo for the “1979” sample, ranging from the innermost areas (close to the mouth of the Verdugo River, the Ría de Vigo’s main river) to the outermost parts (Cabo Home, N; and Baiona, S). The average distance between localities was 2.61 km (SD = 1.99 km). Based on previous results on genetic differentiation in *L. saxatilis* from this area (Rolán-Alvarez et al. 2004; Tirado et al. 2016; Rivas et al. 2018), these distances are big enough to consider populations from different localities as partially genetically isolated.

Samples for the 2022 data were collected in 5 nonconsecutive days between February and March 2022. Based on

Sacchi’s naming of the different localities and their positions as shown in Figure 1 of that article (Sacchi 1979:9), the coordinates of these localities were inferred (see Table 1). Snails were collected in 36 out of 37 localities (see locality dots and numbers in Figures 1B and 2). The remaining population, corresponding with Sacchi’s “Moaña, entro il porto” (Moaña, within the port; 9<sub>N</sub> in our coding system; located between 8<sub>N</sub> and 10<sub>N</sub> in Figures 1B and 2), was also visited, but no *L. saxatilis* were found there, probably due to the expansion of the port since Sacchi’s samplings. Although *L. saxatilis* does not constitute an endangered species and it is very common in intertidal ecosystems throughout the Ría of Vigo, we followed a “reduction” strategy for our sample size (see Russell and Burch 1959), thus significantly reducing the number of snails used (average  $N = 57$ ) in comparison with Sacchi.

The sample was collected using a sampling quadrat (diameter = 60 cm) and following a stratified method. For this, a characterization of the different microhabitats in the localities was performed based on rock type and intertidal zone. Then, the sampling quadrat was placed randomly at different points of the representative littorinid microhabitat, usually the supralittoral zone (most of the times irrespective of rock type). Sampled individuals were picked up from the sampling quadrat, using as many replicates as were necessary until reaching an average number of ~50 snails. The samples were taken alive from the field to the laboratory and then stored at  $-20\text{ }^{\circ}\text{C}$ . The determination of the color of the individuals was based on Dautzenberg and Fischer (1912), as shown in Sacchi (1979; see Figure 1A). According to this classification, 10 different color categories would exist; from these, 9 would be present in the Ría of Vigo: *albida* (white individuals), *fulva* (a wide class of colorations, from grayish-hazel to yellow-straw—or even light brown), *lutea* (yellow, from citrine to golden), *aurantia* (orange), *fusca* (brown to blackish), *nigra* (brilliant-black), *bande* (shells with 2 large dark main bands on a lighter background), *tessellata* (reticulated or checkered tint), and *lineata* (dark lines coinciding with the grooves of the sculpture). The remaining category, *sanguinea*, described as “blood red,” does not exist in the Ría de Vigo. The available evidence for the species in the genus *Littorina* suggests that shell color (both background, bands, and line patterns) is genetically based, with different background colors and ornamentations coded by different alleles in Mendelian unlinked loci (Ekendahl and Johannesson 1997; Kozminsky 2011; Johannesson and Butlin 2017; Gefaell et al. 2023 and references therein). Genomic analyses have revealed that color traits in the Swedish system of *L. saxatilis* are influenced by several chromosome inversions (Westram et al. 2018; Koch et al. 2021), although the details and reach of such influences are yet not known.

Out of the previous qualitative descriptions, RGB categories for each color category were created to aid the assignment process (except for *bande*, *tessellata*, and *lineata*, which are not unicolor and can be diagnosed based on observed ornamentations) (see Sacchi 1979:12). To avoid potential biases derived from frequency expectations for the different 1979 localities, the 2022 samples were classified without knowing the precise frequencies and distributions of colors provided by Sacchi (1979).

### Ecological data sampling

Ecological data for each locality were collected to provide clues on potential environmental factors associated with the

**Table 1** Localities analyzed by Sacchi (1979) and resampled again in 2022, with their corresponding codes and GPS coordinates. Data from the locality 9<sub>N</sub> are not shown, as we did not find snails there (see main text). Distance (m) is the distance from each locality to the river mouth. *N* is the sample size of the color samplings (1979 or 2022). Size (mm) is the average size ( $\pm$  SD) in 15 representative specimens. *H'* is the Shannon index and *D*<sub>Roger</sub> is the divergence between studies in color frequencies by Roger's distance.  $\chi^2$  is the chi-squared test of color frequencies as measured by *D*<sub>Roger</sub> between color samplings. "ns" indicates non-statistical significance, \*\**P* < 0.01, \*\*\**P* < 0.001

Locality	Code	GPS coordinates	Distance (m)	<i>N</i> <sub>1979</sub>	<i>N</i> <sub>2022</sub>	Size (mm)	<i>H'</i> <sub>2022</sub>	<i>H'</i> <sub>1979</sub>	<i>D</i> <sub>Roger</sub>	$\chi^2$
Punta Cabalo	1 <sub>N</sub>	42°19'36.64"N 8°38'10.68"W	6,960	462	58	9.1 ± 2.20	0.86	1.10	0.05	1.9 <sup>ns</sup>
Punta Pereiró	2 <sub>N</sub>	42°19'19.26"N 8°38'50.07"W	8,093	554	52	10.2 ± 1.97	0.80	0.62	0.08	5.9 <sup>ns</sup>
San Adrián	3 <sub>N</sub>	42°18'05.14"N 8°39'20.3"W	11,495	1,368	50	9.4 ± 3.70	1.32	0.90	0.26	395 <sup>***</sup>
Costa San Adrián	4 <sub>N</sub>	42°17'30.05"N 8°39'30.42"W	12,905	486	50	11.2 ± 3.80	1.01	1.36	0.17	53 <sup>***</sup>
Punta Collo de Bestia	5 <sub>N</sub>	42°17'26.07"N 8°40'14.29"W	14,040	1,028	53	11.3 ± 1.49	1.16	0.69	0.12	150 <sup>***</sup>
Borna	6 <sub>N</sub>	42°16'50.75"N 8°41'48.43"W	17,008	1,804	51	6.8 ± 0.94	1.28	1.60	0.25	141 <sup>***</sup>
Punta Arroás	7 <sub>N</sub>	42°16'40.42"N 8°42'25.56"W	18,066	852	57	8.4 ± 0.74	1.78	1.63	0.11	45 <sup>***</sup>
Meira	8 <sub>N</sub>	42°17'0.05"N 8°43'9.46"W	21,307	752	59	10.5 ± 1.94	1.67	1.40	0.30	132 <sup>***</sup>
Praia de Con	10 <sub>N</sub>	42°16'14.13"N 8°44'24.69"W	24,450	846	50	4.8 ± 0.78	2.03	2.11	0.20	101 <sup>***</sup>
Punta Niño Corvo	11 <sub>N</sub>	42°15'47.70"N 8°45'18.60"W	26,019	1,000	64	7.0 ± 1.06	1.19	2.23	0.28	40 <sup>***</sup>
Punta Rodeira	12 <sub>N</sub>	42°15'29.04"N 8°45'56.67"W	27,237	1,250	56	7.0 ± 1.28	0.79	1.62	0.20	57 <sup>***</sup>
Punta Balea	13 <sub>N</sub>	42°15'6.62"N 8°47'17.89"W	30,212	1,220	58	5.5 ± 0.96	0.89	1.78	0.25	62 <sup>***</sup>
Punta Borneira	14 <sub>N</sub>	42°14'48.60"N 8°47'35.73"W	31,018	1,174	48	5.0 ± 0.89	0.29	0.02	0.03	36 <sup>***</sup>
Punta Salgueira	15 <sub>N</sub>	42°15'3.12"N 8°48'15.04"W	32,368	1,064	58	5.5 ± 0.98	0.32	0.08	0.05	61 <sup>***</sup>
Punta Igreixiña	16 <sub>N</sub>	42°15'14.73"N 8°50'3.75"W	36,235	1,200	57	5.7 ± 0.79	0	0	0	-
Punta Subrido	17 <sub>N</sub>	42°14'51.56"N 8°51'47.65"W	40,007	1,822	50	5.3 ± 1.01	0	0	0	-
Cabo Home	18 <sub>N</sub>	42°15'2.18"N 8°52'18.21"W	41,632	1,704	58	5.4 ± 1.03	1.03	0.00	0.19	388 <sup>***</sup>
Muelle Arcade	1 <sub>S</sub>	42°20'17.73"N 8°36'48.03"W	858	1,252	59	9.6 ± 3.57	1.43	0.95	0.31	59 <sup>***</sup>
Punta Puntal	2 <sub>S</sub>	42°20'6.31"N 8°36'52.21"W	1,221	332	73	10.1 ± 1.15	0.71	0.79	0.04	2.9 <sup>ns</sup>
Punta Pesqueira	3 <sub>S</sub>	42°19'46.01"N 8°36'51.01"W	1,982	832	50	8.5 ± 2.95	1.10	0.94	0.11	4.7 <sup>ns</sup>
Cesantes	4 <sub>S</sub>	42°18'57.52"N 8°37'7.82"W	3,915	1,853	63	10.1 ± 1.15	0.93	1.25	0.17	10 <sup>ns</sup>
Punta Soutelo	5 <sub>S</sub>	42°17'17.01"N 8°38'17.26"W	11,631	495	57	10.5 ± 1.93	1.22	1.05	0.31	170 <sup>***</sup>
Cabanas	6 <sub>S</sub>	42°16'53.95"N 8°39'46.13"W	14,253	788	63	9.9 ± 1.71	2.07	1.79	0.26	104 <sup>***</sup>
Punta Cubillo	7 <sub>S</sub>	42°16'08.4"N 8°40'23.8"W	16,061	680	60	9.5 ± 1.23	1.52	1.46	0.53	212 <sup>***</sup>
Areiño	8 <sub>S</sub>	42°15'35.34"N 8°41'56.07"W	18,791	726	48	6.3 ± 1.07	1.62	1.42	0.65	592 <sup>***</sup>
Alcabre	9 <sub>S</sub>	42°13'25.85"N 8°46'19.56"W	28,311	2,118	61	6.7 ± 1.54	1.18	1.13	0.07	139 <sup>***</sup>
Coruxo	10 <sub>S</sub>	42°12'3.21"N 8°47'7.28"W	31,474	1,190	60	5.4 ± 0.98	1.12	0.94	0.06	47 <sup>***</sup>
Canido	11 <sub>S</sub>	42°11'24.75"N 8°48'35.26"W	34,158	852	63	6.0 ± 0.88	1.32	1.95	0.21	69 <sup>***</sup>
Cabo Estai	12 <sub>S</sub>	42°10'57.47"N 8°48'49.55"W	35,432	1,322	54	8.1 ± 1.50	1.53	1.28	0.48	761 <sup>***</sup>
SE Monteferro	13 <sub>S</sub>	42°9'13.61"N 8°50'4.35"W	39,827	696	59	5.7 ± 1.28	0.41	0.70	0.05	4.5 <sup>ns</sup>
SW Monteferro	14 <sub>S</sub>	42°8'52.07"N 8°49'56.00"W	43,863	718	60	5.4 ± 1.18	0.24	0.21	0.02	14 <sup>**</sup>
Panxón	15 <sub>S</sub>	42°8'32.82"N 8°49'33.62"W	44,911	1,030	61	6.8 ± 1.06	0.00	0.39	0.04	3.2 <sup>ns</sup>
Praia América	16 <sub>S</sub>	42°7'32.02"N 8°49'27.14"W	47,616	844	56	4.3 ± 0.56	1.14	1.54	0.34	118 <sup>***</sup>
Santa Marta	17 <sub>S</sub>	42°6'56.26"N 8°50'13.00"W	53,976	1,160	64	7.4 ± 2.10	1.84	1.01	0.18	161 <sup>***</sup>
Punta Tenaza	18 <sub>S</sub>	42°7'34.25"N 8°50'56.89"W	56,305	372	56	6.1 ± 0.88	0	0.72	0.12	8.7 <sup>ns</sup>
Cuncheira	19 <sub>S</sub>	42°7'23.57"N 8°51'6.54"W	57,405	786	53	7.3 ± 1.53	0	0	0	-
Average				1,020 ± 435	57 ± 6		1.0 ± 0.60	1.0 ± 0.64	0.2 ± 0.15	

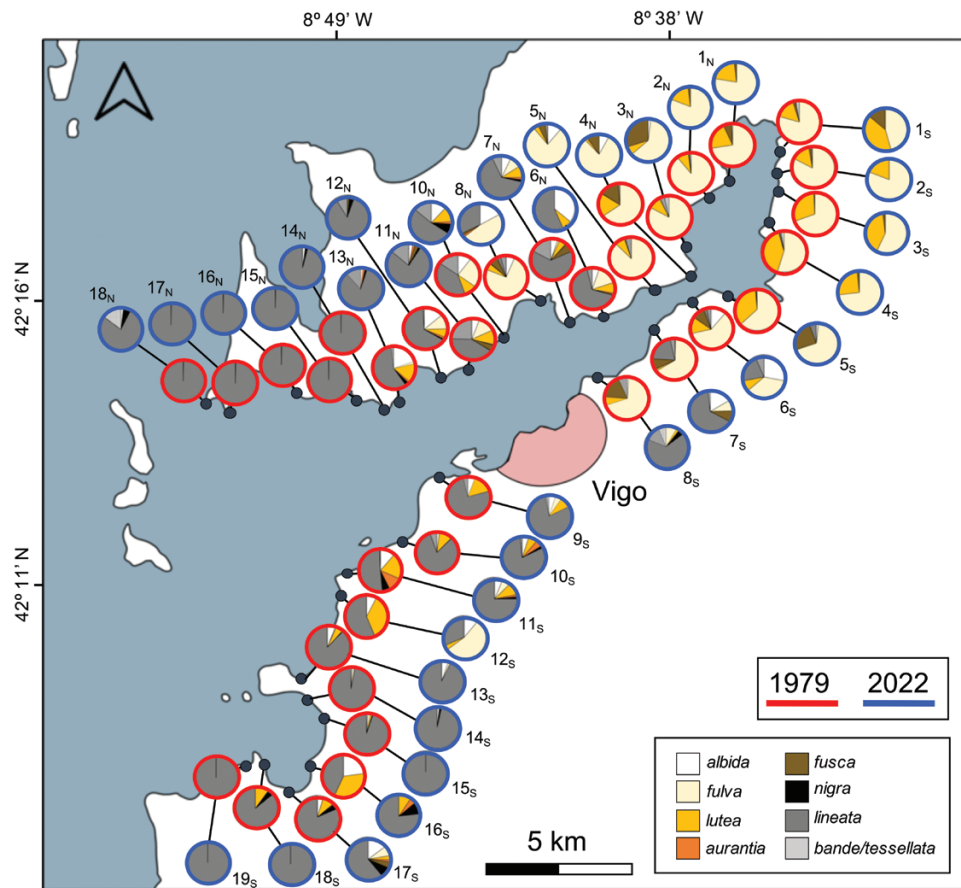


**Figure 2** Pie charts comparing the color frequencies of the different localities along the Ría de Vigo in 1979 and 2022 samples. The map was taken and modified from d-maps (<https://www.d-maps.com>).

color cline. These data were taken on 4 consecutive days during October 2022 using a sampling quadrat (diameter = 60 cm) and following a semiquantitative procedure similar to the Ballantine scale (used to estimate wave exposure; Ballantine 1961; see also Raffaelli and Hawkins 1996; Little et al. 2009). For this, semiquantitative scales and presence/absence classes for key ecological parameters of the intertidal ecosystem were created based on relevant parameters for the Rías Baixas as derived from key published sources (Rolán 1990; Méndez and Vilas 2005; Muñoz Sobrino et al. 2012). Semiquantitative procedures such as the Ballantine scale constitute a useful approach when dealing with large geographical scales (such as the Ría de Vigo; ~41 km bordering the northern coast, and ~57 km the southern coast), and can provide insights into the main ecological trends at play in intertidal ecosystems (Raffaelli and Hawkins 1996; Burrows et al. 2008; Little et al. 2009).

The recorded variables and their corresponding scales for the ecological sampling are presented in Supplementary Table A1 (see online material available). These tried to capture either physical properties (e.g., type of rock, rock size) or ecological parameters like absence/presence or relative abundance of different intertidal species (*Melarhaphé neritoides*, *Monodonta lineata*, *Littorina fabalis/obtusata*, *L. littorea*, barnacle species—mostly *Semibalanus balanoides* and *Chthamalus* sp.—, *Enteromorpha* sp., and *Lichina pygmaea*). These species are unevenly distributed across the Ría, varying mostly according to the degree of wave exposure (Rolán-Alvarez, personal observation). The distance of each locality to the river mouth,

as well as the distance between localities, was also calculated using Google Earth Pro (v. 7.3.6.9285) bordering the coast from the mouth of the Verdugo River to each locality. Given the linearity of the Ría de Vigo, this parameter can be used as an indicator of the degree of wave exposure.

Additionally, the salinity of each locality was estimated using a refractometer (averaged over 2 technical replicates), as previous studies show a clear gradient for this variable from the river mouth to the outermost parts of the Ría de Vigo (Torres López et al. 2001; Souto et al. 2003; Ibánhez et al. 2021). The average shell size (i.e., columella length) was also measured to the nearest 0.1 mm using vernier calipers in a set of 15 specimens selected at random from the 2022 data. Even though Sacchi didn't measure such parameter, size was chosen as a potential indicator of local phenotypic adaptation of *Littorina* species to distinct microhabitats (either by natural selection or phenotypic plasticity; reviewed in Rolán-Alvarez et al. 2015). Previous studies suggest that size might constitute an important trait that affects mortality and is involved in ecotypic evolution (e.g., Boulding et al. 2017). Raw data on color frequencies and ecological parameters are available online (<https://doi.org/10.6084/m9.figshare.21771152.v1>).

### Statistical analyses

Variation in shell color along the Ría de Vigo as well as its potential association with environmental parameters was studied both by comparing shell color frequencies between 1979 and 2022 samples through classical chi-squared tests

and by using a stepwise multiple linear regression of physical and ecological variables on frequencies of the 2 most representative colors of the cline (*fulva* and *lineata*), as well as on the average shell size of *L. saxatilis* for each population. Early in situ inspection revealed that the *fulva* and *lineata* morphs represent the dominant morphs in the innermost and outermost localities of the Ria (respectively), so they can be useful in characterizing the shape of the cline. The stepwise multiple regression used different criteria to introduce ( $P \leq 0.05$ ) or exclude ( $P \geq 0.10$ ) variables into the model.

The Shannon index ( $H'$ ; Shannon 1948; Jain et al. 1975) was used to calculate color-frequency variation at each locality separately for the 1979 and 2022 samples. Shannon index describes the species (or color morph) richness of a community (or a population) as,

$$H' = \sum_{i=1}^S P_i \cdot \log_2 P_i$$

where  $S$  stands for the number of different color morphs, and  $P_i$  is the relative frequency of each color morph. The greater the number of colors at relatively intermediate frequencies, the higher the Shannon index ( $H'$ ). Conversely, monomorphic populations (all individuals showing the same color morph) have  $H' = 0$ . Between-year differences for  $H'$  were analyzed using a fixed-factor ANOVA.

The color-frequency divergence over time (1979 vs. 2022) was analyzed using Roger's genetic distance ( $D_{\text{Roger}}$ ; Rogers 1972; Nei 1987).  $D_{\text{Roger}}$  can also be used to measure discrete variation in a given phenotypic trait, such as color. Roger's distance ( $D_{\text{Roger}}$ ) measures color divergence between populations as,

$$D_{\text{Roger}} = \frac{1}{L} \sqrt{\frac{\sum_u (X_u - Y_u)^2}{2}}$$

where  $L$  stands for the total number of loci-traits (assuming one trait),  $X$  and  $Y$  are the analyzed populations, and  $u$  is the frequency of a given color.  $D_{\text{Roger}} = 0$  is obtained when there is an identical color frequency between populations, and  $D_{\text{Roger}} = 1$  when there exists a complete frequency divergence between them. The significance of  $D_{\text{Roger}}$  was evaluated through chi-squared tests (Sokal and Rohlf 1995). The contribution of each particular color to the former overall distance was estimated using the particular quadratic difference of the previous  $D_{\text{Roger}}$  algorithm per locality and averaged across localities (non-normalized). Differences between colors across the 36 localities were evaluated by one-way ANOVA and the Student–Newman–Keuls (SNK) a posteriori test. All the ecological variables were summarized by means of a principal component analysis (PCA) to test whether they could be interpreted as proxies of wave exposure by latter correlating them with the distance to the river mouth. Statistical analyses were carried out with SPSS v.24 (IBM Corp., USA), and plots were made using R version 4.2.0, with ggplot2 version 3.4.0 for data visualization (Wickham 2016; R Core Team 2022).

## Results

Color frequency, for both 1979 and 2022 samples, shows a clear clinal pattern along the Ría de Vigo from the innermost to the outermost localities (Figure 2). The innermost localities (sheltered and with low salinity) show a high frequency of *fulva* individuals, with frequencies > 50% in most

of them. The outer localities (wave-exposed and relatively high salinity; around 35–36 g of salt per liter/kg of water) show a high frequency of the *lineata* morph, even reaching monomorphism (100%) in many of them. Finally, intermediate localities show high color diversity both in terms of the number of color morphs present at each locality (including *albida*, *lutea*, *aurantia*, or *nigra*) and in terms of the relative frequency of each of these morphs. A significant Pearson's  $r$  correlation exists between the color frequencies of *fulva* and *lineata* morphs and each locality's distance to the river mouth (used as a simple proxy for the degree of wave exposure), irrespective of the data series (1979 vs. 2022): positive for *lineata* 1979 ( $r = 0.83$ ;  $df = 35$ ;  $P < 0.001$ ) and *lineata* 2022 ( $r = 0.83$ ;  $df = 35$ ;  $P < 0.001$ ), and negative for *fulva* 1979 ( $r = -0.82$ ;  $df = 35$ ;  $P < 0.001$ ) and *fulva* 2022 ( $r = -0.73$ ;  $df = 35$ ;  $P < 0.001$ ) (Figure 3). Taken together, these results both support the existence of a color cline in *L. saxatilis*, with 3 different color zones across the Ría de Vigo, as well as its overall maintenance over time.

The mean color biodiversity ( $H'$ ) is also similar between both samples (1979 vs. 2022; Table 1;  $F_{\text{ANOVA}} = 0.1$ ;  $df = 1/70$ ;  $P = 0.875$ ). In addition, there is a high correlation across localities between data samples ( $r = 0.74$ ;  $df = 35$ ;  $P < 0.001$ ). However, putting aside the global pattern of similarity (i.e., stability), some differences also exist between samples, as revealed by  $D_{\text{Roger}}$  and chi-squared tests (Table 1). Averaged divergence per locality between periods is about 20% of the maximum possible ( $D_{\text{Roger}} = 0.20 \pm 0.15$ ), and the frequencies differ significantly in most chi-squared comparisons (25 out of 36; Table 1). The contribution of each color to the  $D_{\text{Roger}}$  distance suggests that this divergence between samples affects preferentially the main clinal colors (i.e., *fulva* and *lineata*; Figure 4), as there were significant differences between colors by ANOVA ( $F = 5.08$ ;  $df = 8/315$ ;  $P < 0.0001$ ). The SNK test identifies 2 significant groups (alpha = 0.05): *fulva* and *lineata* vs. the rest of the colors (Figure 4). In turn, this could be interpreted as an indication that, despite the stability of the overall pattern, the cline has changed during the studied period, resulting in an increased frequency of *lineata* along several intermediate localities (mostly southern) while decreasing that of *fulva* (see Figure 2).

Several potential predictive variables of the clinal color distribution (estimated through *fulva* and *lineata* frequencies) and the average shell size (a characteristic adaptive trait in this species; e.g., Rolán-Alvarez et al. 2015; Boulding et al. 2017) were explored using the stepwise linear multiple regression (Supplementary Table A2, see online material available) to gain insight into potential causal factors. This analysis shows that the 2 colors (both in northern and southern localities) exhibit a strong association with several variables that capture different physical and/or ecological characteristics of the environment (from 1 to 4 variables). We can interpret such variables as proxies of the degree of wave exposure and position along the Ría, as a PCA including all of them yields a PC1 that explains 41% of the variance and that shows a significant correlation with the river mouth ( $r = 0.79$ ,  $P = 0.002$ ; see Burrows et al. 2008 for an analogous use of PCA). In this sense, multiple regression analysis shows that *lineata* frequency is almost fully explained ( $R^2 = 0.97$ ) by 3 variables in the north (including the presence of *Monodonta lineata* and the abundance of *Lichina pygmaea*) but only one (presence of *Melarhappe neritoides*;  $R^2 = 0.69$ ) in the south. On the other hand, *fulva*

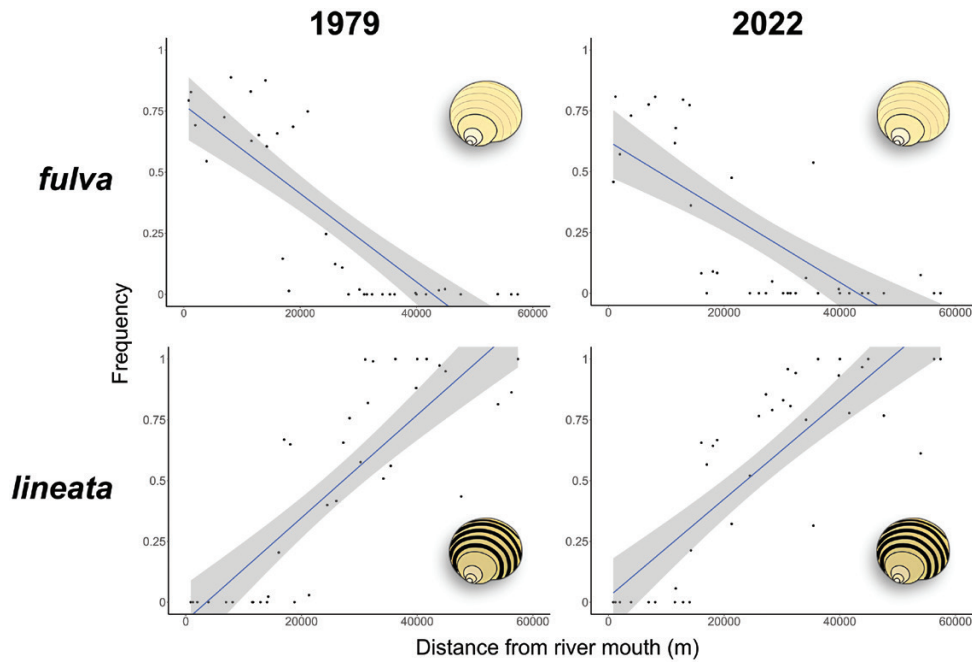


**Figure 3** Frequencies of *fulva* (up) and *lineata* (down) for the 1979 (left) and 2022 (right) samples in relation to the distance from the mouth of the Verdugo River.  $R^2$  coefficients and  $P$ -values for the linear regression corresponding to each figure: for *fulva* 1979 ( $R^2 = 0.67$ ;  $P < 0.001$ ), *fulva* 2022 ( $R^2 = 0.53$ ;  $P < 0.001$ ), *lineata* 1979 ( $R^2 = 0.68$ ;  $P < 0.001$ ), and *lineata* 2022 ( $R^2 = 0.69$ ;  $P < 0.001$ ).

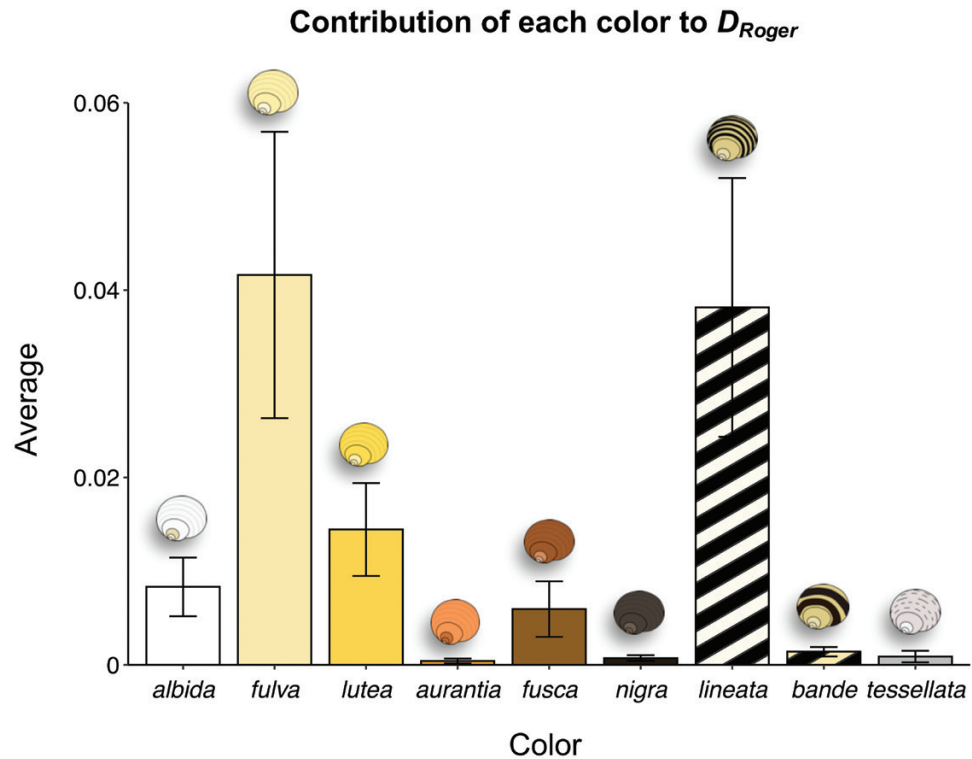


**Figure 4** The contribution of each color to  $D_{Roger}$ , or the average squared difference in color frequency between the 1979 and 2022 samples for each single color morph. The bars represent standard errors.

frequency is fully explained ( $R^2 = 0.98$ ) by 4 variables in the north (absence of *Monodonta lineata*, mean salinity, average rock size, and *Enteromorpha* sp. abundance), while in the south a large portion of variance ( $R^2 = 0.83$ ) is explained by (low) salinity. Interestingly, a trait typically associated with

local adaptation—i.e., size—is fully explained ( $R^2 = 0.97$ ) by 2 variables (presence of *Melarhappe neritoides* and *Enteromorpha* sp. abundance) in the north, and explained ( $R^2 = 0.83$ ) by 2 variables in the south (presence of *Melarhappe neritoides* and *L. littorea*). All explanatory

variables in multiple regression analyses show a clear environmental gradient along the Ría de Vigo, corresponding to the degree of wave exposure.

## Discussion

Our study corroborates the existence of a decades-long color cline in *L. saxatilis* from the Ría de Vigo (Sacchi 1979; Reid 1996). Lab cultures suggest that the Swedish populations of *L. saxatilis* become sexually mature around 6–8 months (Johannesson and Butlin 2017), and although no reliable data exists for the Galician populations, previous simulation studies assume that *L. saxatilis* from this area has a generation time of around 6 months (Fernández-Meirama et al. 2022). This means that it is reasonable to assume that the 46–48 years between both samples analyzed in this study (1979 vs. 2022) are equivalent to around 92–94 generations of *L. saxatilis*. Taken into account that Fischer-Piette and collaborators (Fischer-Piette and Gaillard 1961; Fischer-Piette et al. 1961) already described this color cline in the early 1960s (although they do not provide actual data for comparison with the time series presented in this study; see also Reid 1996), the temporal stability shown in these populations may have lasted for more than 60 years, equivalent to around 120 generations of *L. saxatilis*. Previous studies analyzing the temporal dynamics of color clines suggest that this number of generations might constitute time enough for evolutionary processes to act on populations. For instance, Brakefield and de Jong (2011) show a significant decay in the steepness of a color cline in the 2-spot ladybird (*Adalia bipunctata*) over the course of 50 generations, presumably driven by a genetic response to thermal changes induced by climate change along a 115 km transect in the Netherlands. Cameron et al. (2013) found that in about half the number of these generations, banding morphs of *Cepaea nemoralis* did not change over a cline, while the frequency of the yellow morph increased all over it. Therefore, depending on whether the putative selective pressures acting on a cline vary or not over a given timespan, and whether drift and migration are strong enough to influence the evolutionary outcomes, we might expect changes or stability in the shape of clines across generations.

The other remarkable phenomenon revealed in this study is the variability observed in some populations, despite the overall trend remaining stable over the past decades. We can distinguish between 2 different types of variability: what might be called “local variability” and “directional change.” By local variability we mean the divergence in color frequencies found in specific populations, such as  $10_N$  or  $12_S$  (see Table 1 and Figure 2). Conversely, directional change refers to predictable and recurrent patterns of variation in the frequency of certain morphs. When we compare data from 1979 and 2022, a systematic and recurrent pattern of variation in the *lineata* and *fulva* morphs is observed (*lineata* typically displaces *fulva* in several intermediate-to-inner localities; Figures 2 and 4).

Occasional sampling errors (errors in the geographical correspondence of the sampling sites studied in 1979 and 2022, since Sacchi’s article does not provide any geographic coordinate system to identify exact sampling points), assignment errors, or genetic drift could potentially explain local variability. However, although it cannot be known whether the 2022 sampling points exactly correspond to those of 1979, or whether the assignment process was done using the exact same criteria, we believe that the temporal stability and

directional change observed in this cline between different time series cannot be simply attributed to either sampling or assignment errors, or genetic drift. As for assignment errors, it is virtually impossible to confuse *lineata* and *fulva* ecotypes (the morphs mostly involved in both the temporal stability and directional change of the cline). As for sampling errors or genetic drift, such factors would preferentially affect rare colors (due to the fact that random errors tend to affect lower frequencies most), while the contribution of individual colors to Roger’s distance ( $D_{\text{Roger}}$ ) shows the opposite pattern (more pronounced in *lineata* and *fulva*, the most frequent morphs in the outer and inner localities, respectively; Figure 4). Another possible caveat with respect to the observed patterns has to do with potential seasonality effects. Our 2022 data were taken in different seasons (autumn–winter) than these of 1979 (summer). There are only a few studies so far that have analyzed the seasonal changes in the frequency of snails from the genus *Littorina*, yielding negative results. Ekendahl (1994, 1995) didn’t find any seasonal changes in the frequency of color morphs of the Swedish populations of *L. fabalis*. This researcher found, however, seasonal changes in microhabitat choice. Nevertheless, Carballo et al. (2005) found no seasonal changes in the microdistribution of the Crab and Wave ecotypes of *L. saxatilis* in a 3-year study close to the Ría de Vigo. We cannot formally rule out that seasonal microhabitat changes might have affected the clinal color frequencies compared in this study, but given the above-mentioned study, we believe this is highly unlikely. Therefore, the evidence presented in this study suggests that both the temporal stability observed in the cline and the directional changes detected in certain populations are real, demanding mechanistic explanations.

Regarding the directional change, the *lineata* morph is mostly associated with ecological parameters related to wave exposure and relatively high salinity (in a way similar—but not restricted—to the Crab ecotype; Rolán-Alvarez et al. 2007). The expansion of this color morph to the intermediate zone of the Ría (with a corresponding decrease of *fulva*) could indicate a change in any of such parameters from the outer to the mid localities over the past 46–48 years associated with an expansion of Vigo’s main city of Ría de Vigo. However, no systematic analyses of this possibility have yet been carried out, so future studies should systematically investigate this and related scenarios.

As for the temporal stability of the color cline of *L. saxatilis* in the Ría de Vigo, 2 main hypotheses could be invoked as potential explanatory factors: either the combination of migration and genetic drift or some kind of natural selection along one or more ecological gradients (e.g., Mayr 1963; Endler 1977; Ridley 2004; Sætre and Ravinet 2019). We believe that such stability in a clinal pattern is unlikely to be explained through the combination of migration and genetic drift, as such mechanisms predict a much greater degree of stochasticity. Moreover, the cline described in this study shows not only temporal stability but also spatial replication. Considering the low dispersal capacity of *L. saxatilis* (Rolán-Alvarez et al. 2015), it is highly unlikely that there is strong genetic connectivity between its northern and southern populations. This suggests that both clinal trends (north and south) are maintained independently through non-stochastic forces, and may qualify as separate spatial replicas. Furthermore, such a clinal pattern has been described in other Rías from the Rías Baixas (Reid 1996; Fischer-Piette and Gaillard 1961; Fischer-Piette



et al. 1961; Rolán-Alvarez, personal observation). Although the genetic structure and connectivity between the northern and southern populations of *L. saxatilis* from the Ría de Vigo should be studied through different genetic markers to formally rule out the migration plus drift hypothesis (e.g., as in Westram et al. 2018), we believe that this is an a priori less convincing scenario.

A much more plausible explanatory mechanism might involve some form of natural selection. In addition to the temporal stability and spatial replication of the cline (which by its own right might already suggest the action of selective forces; Endler 1986), the main reason for this is that there are strong environmental gradients (e.g., temperature, salinity, CO<sub>2</sub>, and wave exposure) along the Ría de Vigo that go parallel to the color cline (Ruiz-Villareal et al. 2002; Gago et al. 2003; Muñoz Sobrino et al. 2012; Ibánhez et al. 2021). These environmental gradients might give rise to differential selective pressures that end up maintaining the cline in a relatively stable form.

Furthermore, multiple regression analyses show that several key ecological variables can explain the observed color distribution, thereby strengthening the case for natural selection. The *lineata* and *fulva* color clines are clearly explained by a few ecological or physical variables that show gradients from inner to outer localities. For example, *Monodonta lineata*, *Melarhaphé neritoides*, and *Lichina pygmaea* tend to be associated with moderate to highly wave-exposed rocky shore areas (Ballantine 1961; Rolán 1990; Burrows et al. 2008), and they show concomitantly positive regression coefficients when explaining the *lineata* clines, whereas, for instance, *Monodonta lineata* shows a negative regression coefficient when explaining the *fulva* ones. The degree of wave exposure might be linked to differences in temperature or salinity, which in turn might constitute powerful selective agents. In the case of temperature, for instance, Phifer-Rixey et al. (2008) provide experimental evidence that thermal stress tolerance might be driving a color cline in *L. obtusata* from the Gulf of Maine. As for salinity, which also shows a concentration gradient over the Ría (e.g., Muñoz Sobrino et al. 2012; this study), its positive regression coefficients with *lineata* frequency and negative with *fulva* frequency suggest that it constitutes another selective pressure operating along the cline. In this sense, previous experimental evidence exists that the different color morphs of *L. saxatilis* from the White Sea have different saline-stress tolerance (Sokolova and Berger 2000), although the molecular mechanisms for such association are not known yet (see also Minton and Gunderson 2001 for a similar case in a different gastropod species). If that would be the case, then shell color would not be the primary target of selection, but only a correlated trait genetically associated with saline-stress resistance (or other biotic or abiotic factors) genes. This genetic association would not be surprising, as genomic data suggest that in *L. saxatilis* chromosomal inversions may contain several loci involved in adaptive traits, thereby contributing to low recombination between them (Koch et al. 2021).

As for the explanation of cline formation, 2 different mechanisms have been put forward: primary differentiation and secondary contact (Endler 1977). Spatial heterogeneity of a formerly homogenous environment leads to cline formation by primary differentiation. A similar primary differentiation scenario can be achieved through the colonization of a novel environment with distinctive

characteristics by a species hitherto confined to a homogeneous area. In our case, the latter primary differentiation scenario is a priori supported by the historical geomorphology of the Ría de Vigo: before the early Holocene sea-level rise (12,000–7,000 years ago), sea level at this location was about 30–35 m below the current level, with the Ría de Vigo forming a river valley and the coast being located to the west of the Cíes Islands (Costas et al. 2009). As the sea level rose, marine water inundated the river valley, thereby gradually giving rise to the different zones (exterior, intermediate, and interior; in that order) of the Ría. It is possible, therefore, that from that point on populations of *L. saxatilis* began to colonize the intermediate and inner zones of the Ría, thereby being exposed to different selective pressures. An alternative hypothesis on the formation of the color cline observed in this study is viewing it as the product of a secondary contact between 2 distinct ecotypes (*lineata* and *fulva*) that differ in shell color and a suit of related traits, and that are locally adapted to the different ends of a temperature, salinity, and/or wave exposure gradient. Under this scenario, both ecotypes would show at least partial reproductive isolation between them, and the intermediate zone of the Ría would constitute a hybrid zone with a more or less steep cline in traits and allele frequencies, depending on the strength of divergent selection (as in the Crab and Wave ecotypes; see Westram et al. 2018). Although this latter scenario fits worst with historical geomorphology than the former, future studies on DNA markers and experimental settings should be put in place to reveal which of them is the correct one and which selective agents might constitute the causal mechanisms of this decades-long clinal pattern in a marine snail.

## Acknowledgments

The authors thank Mary Riádigos for her administrative support, Sabela Cordeiro for her assistance during fieldwork, and 4 anonymous referees for their constructive criticism on the early version of this manuscript.

## Funding

This work has received financial support from the Ministerio de Ciencia e Innovación (PID2021-124930NB-I00), Xunta de Galicia (GRC, ED431C 2020-05), Centro singular de Investigación de Galicia accreditation 2019–2022, and the European Union (European Regional Development Fund—ERDF). Juan Galindo was funded by a JIN project (Jóvenes Investigadores, Ministerio de Ciencia, Innovación y Universidades, RTI2018-101274-J-I00). Juan Gefaell was funded by a Xunta de Galicia Predoctoral Research Contract (ED481A-2021/274).

## Conflict of Interest

The authors declare that they have no conflict of interest.

## Supplementary Material

Supplementary material can be found at <https://academic.oup.com/cz>.

## References

- Abalos J, 2021. *The Functional Significance of Colour Polymorphism in the European Common Wall Lizard Podarcis muralis*. PhD dissertation. Valencia: Universitat de València.
- Antoniazza S, Burri R, Fumagalli L, Goudet J, Roulin A, 2010. Local adaptation maintains clinal variation in melanin-based coloration of European barn owls *Tyto alba*. *Evolution* 64:1944–1954.
- Ballantine WJ, 1961. A biologically-defined exposure scale for the comparative description of rocky shores. *Field Stud* 1:1–19.
- Boulding EG, Rivas MJ, González-Lavín N, Rolán-Alvarez E, Galindo J, 2017. Size selection by a gape-limited predator of a marine snail: Insights into magic traits for speciation. *Ecol Evol* 7:674–688.
- Brakefield PM, de Jong PW, 2011. A steep cline in ladybird melanism has decayed over 25 years: A genetic response to climate change? *Heredity* 107:574–578.
- Burrows MT, Harvey R, Robb L, 2008. Wave exposure indices from digital coastlines and the prediction of rocky shore community structure. *Mar Ecol Prog Ser* 353:1–12.
- Cameron RAD, Cook LM, Greenwood JJD, 2013. Change and stability in a steep morph-frequency cline in the snail *Cepaea nemoralis* (L.) over 43 years. *Biol J Linn Soc* 108:473–483.
- Carballo M, Caballero A, Rolán-Alvarez E, 2005. Habitat-dependent ecotype micro-distribution at the mid-shore in natural populations of *Littorina saxatilis*. *Hydrobiologia* 548:307–311.
- Consentino BJ, Moore JD, Karraker NE, Ouellet M, Gibbs JP, 2017. Evolutionary response to global change: Climate and land use interact to shape color polymorphism in a woodland salamander. *Ecol Evol* 7:5426–5434.
- Cook LM, 2017. Reflections on molluscan shell polymorphisms. *Biol J Linn Soc* 121:717–730.
- Cook LM, Cowie RH, Jones JS, 1999. Change in morph frequency in the snail *Cepaea nemoralis* on the Marlborough Downs. *Heredity* 82:336–342.
- Cook LM, Pettitt CWA, 1998. Morph frequencies in the snail *Cepaea nemoralis*: Changes with time and their interpretation. *Biol J Linn Soc* 64:137–150.
- Cook LM, Riley AM, Woiwod IP, 2002. Melanic frequencies in three species of moths in post industrial Britain. *Biol J Linn Soc* 75:475–482.
- Cooper IA, 2010. Ecology of sexual dimorphism and clinal variation of coloration in a damselfly. *Am Nat* 176:566–572.
- Costas S, Muñoz Sobrino C, Alejo I, Pérez-Arlucea M, 2009. Holocene evolution of a rock-bounded barrier-lagoon system, Cíes Islands, northwest Iberia. *Earth Surf Process Landforms* 34:1575–1586.
- Dautzenberg PH, Fischer H, 1912. Mollusques provenant des campagnes de l'«Hirondelle» et de la «Princesse Alice» dans les mers du Nord. *Rés Campagnes Scientif Prince Albert de Monaco* 37:1–619.
- Davison A, Jackson HJ, Murphy EW, Reader T, 2019. Discrete or indiscrete? Redefining the colour polymorphism of the land snail *Cepaea nemoralis*. *Heredity* 123:162–175.
- de Jong PW, Brakefield PM, 1998. Climate and change in clines for melanism in the two-spot ladybird *Adalia bipunctata* (Coleoptera: Coccinellidae). *Proc Biol Sci* 265:39–43.
- Dearn JM, 1981. Latitudinal cline in a colour pattern polymorphism in the Australian grasshopper *Phaulacridium vittatum*. *Heredity* 47:111–119.
- Dearn JM, 1990. Color pattern polymorphism. In: Chapman RF, Joern A, editors. *Biology of Grasshoppers*. New York: John Wiley & Sons, 517–549.
- Ekendahl A, 1994. Factors important to the distribution of colour morphs of *Littorina mariae* Sacchi & Rastelli in a non-tidal area. *Ophelia* 40:1–12.
- Ekendahl A, 1995. Microdistribution in the field and habitat choice in aquaria by colour morphs of *Littorina mariae* Sacchi & Rastelli. *J Molluscan Stud* 61:249–256.
- Ekendahl A, Johannesson K, 1997. Shell color variation in *Littorina saxatilis* Olivi (Prosobranchia: Littorinidae): a multi-factor approach. *Biol J Linn Soc* 62:401–419.
- Endler JA, 1977. *Geographic Variation, Speciation, and Clines*. *Monographs in Population Biology*, vol. 10. Princeton: Princeton University Press.
- Endler JA, 1986. *Natural Selection in the Wild*. *Monographs in Population Biology*, vol. 21. Princeton: Princeton University Press.
- Evans AE, Forester BR, Jockusch EL, Urban MC, 2018. Salamander morph frequencies do not evolve as predicted in response to 40 years of climate change. *Ecography* 41:1687–1697.
- Fernández-Meirama M, Rolán-Alvarez E, Carvajal-Rodríguez A, 2022. A simulation study of the ecological speciation conditions in the Galician marine snail *Littorina saxatilis*. *Front Gen* 13:680792. doi:10.3389/fgene.2022.680792
- Fischer-Piette E, Gaillard JM, 1961. Études sur les variations de *Littorina saxatilis*. III. Comparaison des points abrités au long des côtes françaises et ibériques. *Bull Soc Zool France* 86:163–172.
- Fischer-Piette E, Gaillard JM, Jouin C, 1961. Études sur les variations de *Littorina saxatilis*. IV. Comparaison de les points battus, au long des côtes européennes. A. Côtes ibériques. *Bull Soc Zool France* 86:320–328.
- Gago J, Gilcoto M, Pérez FF, Ríos AF, 2003. Short-term variability of  $f\text{CO}_2$  in seawater and air-sea  $\text{CO}_2$  in a coastal upwelling system (Ría de Vigo, NW Spain). *Mar Chem* 80:247–264.
- Galeotti P, Rubolini D, Dunn PO, Fasola M, 2003. Colour polymorphism in birds: Causes and functions. *J Evol Biol* 16:635–646.
- Galindo J, Gefaell J, Morán P, Rolán-Alvarez E, 2020. Inferring fast ecotypic divergence in a protected marine area: Comparing  $Q_{st}$  and  $F_{st}$  patterns in *Littorina saxatilis* subpopulations from Cíes Islands in Spain. *Mar Biol* 167:103.
- Gefaell J, Galindo J, Rolán-Alvarez E, 2023. Shell color polymorphism in marine gastropods. *Evol Appl* 16:202–222.
- Hantak MM, Federico NA, Blackburn DC, Guralnick RP, 2021. Rapid phenotypic change in a polymorphic salamander over 43 years. *Sci Rep* 11:22681.
- Hoffman EA, Blouin MS, 2000. A review of colour and pattern polymorphisms in anurans. *Biol J Linn Soc* 70:633–665.
- Ibáñez JSP, Álvarez-Salgado XA, Nieto-Cid M, Rocha C, 2021. Fresh and saline submarine groundwater discharge in a large coastal inlet affected by seasonal upwelling. *Limnol Oceanogr* 66:2141–2158.
- Jain SK, Qualset CO, Bhatt GM, Wu KK, 1975. Geographical patterns of phenotypic diversity in a world collection of durum wheats. *Crop Sci* 15:700–704.
- Johannesson K, 2015. What can be learnt from a snail? *Evol Appl* 9:153–165.
- Johannesson K, Butlin RK, 2017. What explains rare and conspicuous colours in a snail? A test of time-series data against models of drift, migration or selection. *Heredity* 118:21–30.
- Johannesson K, Butlin RK, Panova M, Westram AM, 2017. Mechanisms of adaptive divergence and speciation in *Littorina saxatilis*: Integrating knowledge from ecology and genetics with new data emerging from genomic studies. In: Oleksiak MF, Rajora OP, editors. *Population Genomics: Marine Organisms*. New York: Springer. 277–301.
- Koch EL, Morales HE, Larsson J, Westram AM, Faria R et al., 2021. Genetic variation for adaptive traits is associated with polymorphic inversions in *Littorina saxatilis*. *Evol Lett* 5:196–213.
- Köhler G, Samietz J, Schielzeth H, 2017. Morphological and colour morph clines along an altitudinal gradient in the meadow grasshopper *Pseudochorthippus parallelus*. *PLoS One* 12:e0189815.
- Kozminsky EV, 2011. Inheritance of longitudinal shell bands in the snails *Littorina obtusata* and *L. saxatilis* (Gastropoda, Prosobranchia). *Russ J Gen* 47:1112–1119.
- Little C, Williams GA, Trowbridge CD, 2009. *The Biology of Rocky Shores*. 2nd edn. Oxford: Oxford University Press.
- Magnúsdóttir H, Pálsson S, Westfall KM, Jónsson ZO, Örnólfsson EB, 2018. Shell morphology and color of the subtidal whelk *Buccium undatum* exhibit fine-scaled spatial patterns. *Ecol Evol* 8:4552–4563.
- Mayr E, 1963. *Animal Species and Evolution*. Cambridge (MA): The Belknap Press.

- Méndez G, Vilas F, 2005. Geological antecedents of the Rias Baixas (Galicia, northwest Iberian Peninsula). *J Mar Syst* 54:195–207.
- Minton RL, Gunderson RW, 2001. *Puperita tristis* (d'Orbigny, 1842) (Gastropoda: Neritidae) is an ecotype of *Puperita pupa* (Linnaeus, 1767). *Am Malacol Bull* 16:13–20.
- Mullen LM, Hoekstra HE, 2008. Natural selection along an environmental gradient: A classic cline in mouse pigmentation. *Evolution* 62:1555–1570.
- Muñoz Sobrino C, García-Gil S, Iglesias J, Martínez Carreño N, Ferreiro Da Costa J et al., 2012. Environmental change in the Ría de Vigo, NW Iberia, since the mid-Holocene: New paleoecological and seismic evidence. *Boreas* 41:578–601.
- Nei M, 1987. *Molecular Evolutionary Genetics*. New York: Columbia University Press.
- Oxford GS, Gillespie RG, 1998. Evolution and ecology of spider coloration. *Annu Rev Entomol* 43:619–643.
- Ožgo M, Schilthuizen M, 2012. Evolutionary change in *Cepaea nemoralis* shell colour over 43 years. *Glob Chang Biol* 18:74–81.
- Phifer-Rixey M, Heckman M, Trussell GC, Schmidt PS, 2008. Maintenance of clinal variation for shell colour phenotype in the flat periwinkle *Littorina obtusata*. *J Evol Biol* 21:966–978.
- R Core Team, 2022. *R: A Language and Environment for Statistical Computing*. Vienna: R Foundation for Statistical Computing. <https://www.R-project.org/>.
- Raffaelli D, Hawkins S, 1996. *Intertidal Ecology*. London: Chapman and Hall.
- Ramos-Gonzalez D, Davison A, 2021. Qualitative and quantitative methods show stability in patterns of *Cepaea nemoralis* shell polymorphism in the Pyrenees over five decades. *Ecol Evol* 11:6167–6183.
- Reid DG, 1996. *Systematics and evolution of Littorina*. Andover: The Ray Society.
- Ridley M, 2004. *Evolution*. 3rd edn. London: Blackwell.
- Rivas MJ, Saura M, Pérez-Figueroa A, Panova M, Johansson T et al., 2018. Population genomics of parallel evolution in gene expression and gene sequence during ecological adaptation. *Sci Rep* 8:16147.
- Rogers JS, 1972. Measures of genetic similarity and genetic distance. In: *Studies in Genetics VII*. Austin: University of Texas Publication. 145–153.
- Rolán E, 1990. *Moluscos de la Ría de Vigo, Vol. I: Gasterópodos*. Santiago de Compostela: Universidade de Santiago de Compostela, Servicio de Publicaciones e Intercambio Científico.
- Rolán-Alvarez E, 2007. Sympatric speciation as a by-product of ecological adaptation in the Galician *Littorina saxatilis* hybrid zone. *J Molluscan Stud* 73:1–10.
- Rolán-Alvarez E, Austin CJ, Boulding EG, 2015. The contribution of the genus *Littorina* to the field of evolutionary ecology. In: Hughes RN, Hughes DJ, Smith IP, Dale AC, editors. *Oceanography and Marine Biology: An Annual Review*, Vol. 53. Boca Ratón: CRC Press. 157–214.
- Rolán-Alvarez E, Carballo M, Galindo J, Morán P, Fernández B et al., 2004. Nonallopatric and parallel origin of local reproductive barriers between two snail ecotypes. *Mol Ecol* 13:3415–3424.
- Roulin A, 2014. Melanin-based colour polymorphism responding to climate change. *Glob Chang Biol* 20:3344–3350.
- Ruiz-Villareal M, Montero P, Taboada JJ, Prego R, Leitão P et al., 2002. Hydrodynamic model study of the Ría de Pontevedra under estuarine conditions. *Estuar Coast Shelf Sci* 54:101–113.
- Russell WMS, Burch RL, 1959. *The Principles of Humane Experimental Technique*. London: Methuen.
- Saccheri IJ, Roussett F, Watts PC, Brakefield PM, Cook LM, 2008. Selection and gene flow on a diminishing cline of melanic peppered moths. *Proc Natl Acad Sci U S A* 105:16212–16217.
- Sacchi CF, 1979. Frequenze di fenotipi cromatici in *Littorina saxatilis* (Olivi) della Ría di Vigo (Spagna Nordoccidentale) e loro significato ecologico. *Natura* 70:7–21.
- Sacchi CF, Malcevschi S, 1983. Polimorfismo ed ambiente nel proso-branco intermareale *Littorina saxatilis* (Olivi) dei dintorni di Vigo (Galizia, Spagna Nordoccidentale). *Boll Mus Civ Stor Nat Venezia* 33:7–21.
- Sætre GP, Ravinet M, 2019. *Evolutionary Genetics*. Oxford: Oxford University Press.
- Shannon CE, 1948. A mathematical theory of communication. *Bell Syst Tech J* 27:379–423.
- Smith TM, Smith RL, 2012. *Elements of Ecology*. 8th edn. New York: Pearson.
- Sokal RR, Rohlf FJ, 1995. *Biometry*. 3rd edn. New York: W. H. Freeman & Co.
- Sokolova IM, Berger VJ, 2000. Physiological variation related to shell color polymorphism in White Sea *Littorina saxatilis*. *J Exp Mar Biol Ecol* 245:1–23.
- Souto C, Gilcoto M, Fariña-Busto L, Pérez FF, 2003. Modeling the residual circulation of a coastal embayment affected by wind-driven upwelling: circulation of the Ría de Vigo (NW Spain). *J Geophys Res* 108:3340.
- Suárez-Tovar CM, Guillermo-Ferreira R, Cooper IA, Cezário RR, Córdoba-Aguilar A, 2022. Dragon colors: The nature and function of Odonata (dragonfly and damselfly) coloration. *J Zool* 317:1–9.
- Takahashi Y, Morita S, Yoshimura J, Watanabe M, 2011. A geographic cline induced by negative frequency-dependent selection. *BMC Evol Biol* 11:256.
- Tirado T, Saura M, Rolán-Alvarez E, Quesada H, 2016. Historical biogeography of the marine snail *Littorina saxatilis* inferred from haplotype and shell morphology evolution in NW Spain. *PLoS One* 11:e0161287.
- Torres López S, Varela RA, Delhez E, 2001. Residual circulation and thermohaline distribution of the Ría de Vigo: A 3-D hydrodynamical model. *Sci Mar* 65:277–289.
- Westram AM, Rafajlović M, Chaube P, Faria R, Larsson T et al., 2018. Clines on the seashore: the genomic architecture underlying rapid divergence in the face of gene flow. *Evol Lett* 2:297–309.
- Wickham H, 2016. *ggplot2: Elegant Graphics for Data Analysis*. New York: Springer-Verlag.
- Wolda H, 1969. Stability of a steep cline in morph frequencies of the snail *Cepaea nemoralis* (L.). *J Anim Ecol* 38:623–635.